Two-dimensional Inversion of Resistivity and IP Data with Topography

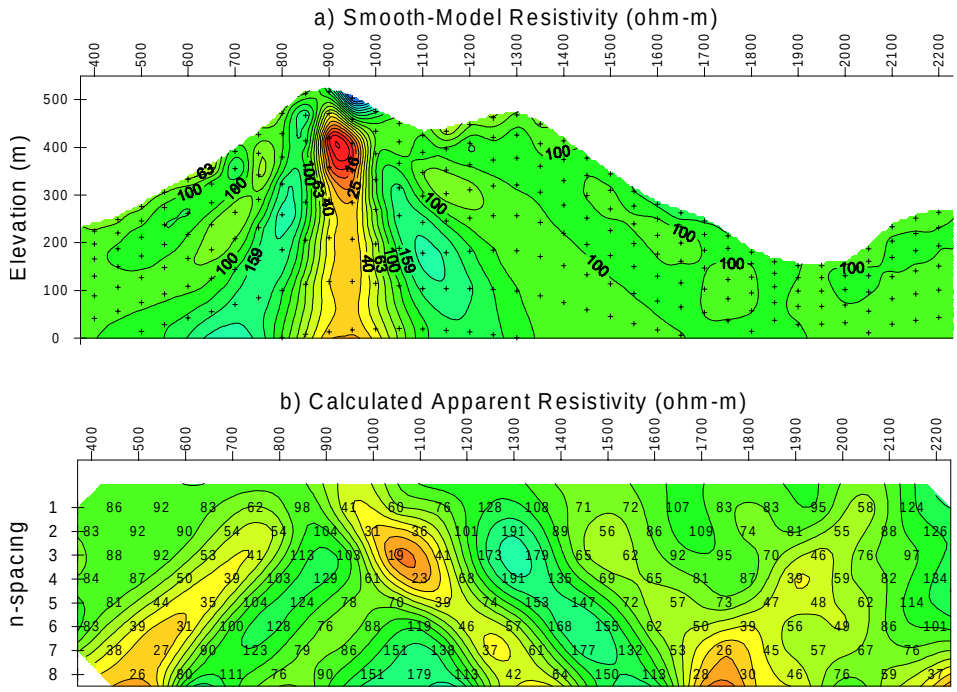

by

Scott MacInnes
Geophysicist
Zonge Engineering and Research
Tucson, Arizona

and

Ken Zonge
President
Zonge Engineering and Research
Tucson, Arizona

Presented at the 102 Annual
Northwest Mining Association Convention
Session Geophysics/Geochemistry 1
Spokane, Washington
December 3-6, 1996

Abstract

Two-dimensional, smooth-model inversion of resistivity and induced polarization data produces image-like, electrical property sections which improve the data's interpretability. Recent software improvements enable routine smooth-model inversion of resistivity and induced polarization (IP) data. Nearly uniform starting models are generated by running broad moving-average filters over lines of dipole-dipole or pole-dipole data. Model resistivity and IP properties are then adjusted iteratively until calculated data values match observed values as closely as possible, given constraints which keep the model section smooth. Calculated values are generated with a finite element algorithm which can be adapted for accurate two-dimensional modeling of data collected in rough terrain. Smooth-model inversion of sample data show the method's utility as an interpretation aid and the importance of modeling topography in areas with significant relief.

Introduction

Resistivity and IP data are usually plotted in pseudosections which place apparent resistivity and IP values in positions which correspond to each value's lateral location and approximate depth of investigation. Pseudosections do not create particularly good images of subsurface structure. Pseudosections of dipole-dipole or pole-dipole data measured over compact objects have wide triangular features, sometimes with the appearance of a pair of pant legs. Pant-leg artifacts are often overlapping, making interpretation difficult. Although attempts have been made to improve the pseudosection presentation by adjusting plot point depths (Edwards, 1977), pant-leg artifacts remain. Smooth-model inversion is an approach which allows routine processing of resistivity and IP data to produce an image of subsurface electrical properties without the pant-leg artifacts present in pseudosections.

Several authors have presented algorithms for smooth-model inversion of resistivity/IP data. Oldenburg and Li (1994) describe smooth-model inversion of resistivity/IP data using a finite-difference forward modeling algorithm. Their treatment is very complete, but finite-difference modeling requires a rectangular mesh which cannot be distorted to match irregular terrain, limiting its accuracy for topographic modeling. Loke and Barker (1996) also use finite-difference modeling in a smooth-model inversion program used to process apparent resistivity data. Yong and Wang (1990) describe the incorporation of topography into a two-dimensional resistivity inversion, but require selection of model body boundaries before inversion rather than using smoothness constraints to generate an image section. The smooth-model algorithm described here extends previous work by using a finite-element algorithm to include accurate modeling of two-dimensional topography along with subsurface resistivity and IP. Data are inverted iteratively using both a-priori-model and model-smoothness constraints. Computer programs described by Tripp, Hohmann and Swift (1984) and Wannamaker (1992) were extended to allow distortion of the finite-element mesh to follow topography and inversion with smoothness constraints of large model sections. Several examples are presented to show the utility of resistivity/IP smooth-model inversion in general and the importance of modeling topographic effects in areas with rough terrain in particular.

Smooth-Model Inversion

There is currently no direct way of going directly from a set of resistivity/IP measurements to a model section. There are also many possible models which can produce a particular resistivity/IP data set. Forward modeling algorithms, such as finite elements, can be used to calculate resistivity/IP data, given a particular model section and array configuration. Given a set of indirect measurements, inversion procedures attempt to find a model section which matches observed data. Since many model sections will produce calculated data matching an observed data set, constraints are necessary to control model characteristics. Smoothness constraints generate the smoothest model which also fits observed data to an acceptable level. A priori constraints search for an inversion model as close as possible to a model based on independent geologic information, while fitting observed data to an acceptable level. Multiple constraint sets can be used. The smooth-model inversion described here attempts simultaneously minimize the squared difference between observed and calculated data, the squared difference between an arbitrary a priori and inverted model and a measure of inverse model roughness. Tradeoffs between

these conflicting goals can be varied by adjusting weights given to matching observed data, staying close to a priori model values, or keeping the inversion model smooth. A model section is represented by an array of resistivity and IP phase or chargeability values with a fixed number of rows and columns. For data sets collected over rough terrain, the model-section array can be distorted to follow irregular topography. An a-priori model is generated by assigning resistivity and IP values to each node in the array and the a priori model is usually used to start the inversion. A-priori-model values are usually generated by running a broad moving-average filter over observed apparent resistivity and IP pseudosections, but if available, geologic information from drilling, mapping or other geophysical surveys can be incorporated into the a priori model. Inversion proceeds iteratively, apparent resistivities are completely inverted first, followed by a separate inversion of IP data. A two-dimensional finite-element algorithm is used to calculate the direct-current response of the current model section and the sensitivity of calculated values to perturbations in model parameters. At each iteration, the difference between observed and calculated data are determined along with measures of how well the current inversion model fits constraints, then improved model parameters are estimated for the next iteration. Since an a priori starting model can be generated by filtering observed data, smooth-model inversion can proceed without selecting a geologic model ahead of time, making it useful as an automated imaging tool. Smooth-model inversion of a dipole-dipole line with fifty points takes about five minutes on a 90 MHz Pentium personal computer, so the approach is fast enough for routine use, making it a practical automated imaging tool.

North Silver Bell Line 0

To illustrate smooth-model inversion, data from an resistivity/IP line over a porphyry copper deposit are inverted. 500 foot dipole-dipole resistivity/IP data from North Silver Bell near Tucson, Arizona are shown in figure 1. There is a broad area of lower apparent resistivity on the western half of the pseudosection and a strong pant-leg feature in IP phase, but surface features obscure deeper structure. A starting model was generated by moving-average filtering of the apparent resistivity and IP pseudosections, followed by inversion to the smooth models shown in figure 2. Calculated apparent resistivity and IP data for the inverted model closely matches observed data (figure 3). Smooth-model resistivity shows a low resistivity layer which closely tracks a supergene enrichment zone (figure 2a) extending from 1200E to 6200E. A west dipping layer of high smooth-model IP phase at 5200E maps phyllic alteration underneath the supergene enrichment (figure 2b). Inversion also produces estimates of model error, which are useful in determining a survey's maximum depth of investigation. Figure 4 shows smooth-model error for inversion of the North Silver Bell data. A sharp increase in model smooth-model resistivity and IP phase error at the 1000 foot elevation maps the survey's maximum depth of investigation.

The tradeoff between fitting observed data versus smoothness constraints can be optimized by changing the relative weight given smoothness constraints during inversion. Figure 5 shows a curve mapping the tradeoff between fitting observed data and keeping the inversion model smooth. Giving smoothness constraints a large weight (smoothness weighting = 40) produces a very smooth model with does not fit observed data particularly well. Inverting with smoothness constraints given a low weight (smoothness weighting = 0.2) produces a good fit to observed data, but a rough model section. A more optimal choice of constraint weighting (smoothness weighting = 2) balances the tradeoff, achieving a fairly good fit to observed data with the calculated response from a fairly smooth inversion model.

Modeling a Fault Scarp

Dipole-dipole resistivity surveys are often used for answering questions in engineering or environmental studies. Dahlin (1996) describes applications of two-dimensional resistivity surveying to engineering and environmental problems in Europe. Tong and Yang (1990) use inversion of dipole-dipole data to distinguish between a fault scarp and a river terrace. In some situations, a fault scarp could be interpreted as a river terrace, requiring subsurface information to distinguish between two geologic models. An adaptation of Tong and Yang's example is shown in figure 6a, where a normal fault is represented by a vertical 75m offset in otherwise uniform 100 ohm-m basement rock. Basement rocks are covered by a 20 ohm-m alluvial layer, with the fault's location marked by an eroded scarp. Dipole-dipole apparent resistivity data were calculated for this example using a two-dimensional finite-element forward modeling program. Figure 6b is a pseudosection showing 100 m dipole-dipole data calculated

along a line perpendicular to the fault. Apparent resistivity values for n-spacings of one to eight are plotted along a two km line segment centered on the fault scarp. This synthetic example illustrates the utility of dipole-dipole resistivity in imaging subsurface structure and the importance of including topography in the modeling when inverting data taken along lines with topographic relief.

Smooth-model inversion of the normal-fault data set without including topography produces the smooth-model section shown in figure 7a. Away from the fault scarp, the surface alluvial layer is modeled correctly as a steep low-over-high resistivity gradient centered at a depth of 100 m. Both alluvial and basement resistivities are partially recovered, but topographic effects create extra structure in the smooth model near the fault scarp. In terms of imaging, smooth-model inversion without any topographic modeling is a significant improvement over the original pseudosection, but topographic effects degrade imaging of basement structure.

Dipole-dipole apparent resistivity data are sometimes "corrected" for topographic effects in a procedure independent from inversion or interpretation. Topographic effects can be approximated with a forward model using a uniform background resistivity. The ratio of calculated apparent resistivity to model background resistivity can then be used to normalize observed values in a topographic "correction". Correcting for topographic effects before inversion does not allow modeling of the interaction between topography and subsurface resistivity structure, since the model resistivity is set to a uniform value. Figure 8b is a pseudosection of apparent resistivity values calculated for a model with the fault scarp's topography, but with a uniform one ohm-m model resistivity. Figure 8c is a pseudosection of topography-corrected apparent resistivity data created by dividing the original fault scarp values (figure 8a) by predicted topographic effects (figure 8b). Near the fault, topographic-corrected apparent resistivities have the same anomaly shape as uncorrected values, but the anomaly's amplitude has been reduced.

Figure 9a depicts a smooth-model section after inversion of topography-corrected apparent resistivity data. There is improved resolution of the low-over-high resistivity layering along the full length of the section. Both basement and alluvial cover resistivities are imaged much more uniformly. There is a basement unit offset centered on the fault's location, but there is an extra undulation in the basement surface just left of the fault. Correcting topographic effects in a separate step before smooth-model inversion is an improvement over inversion of data with no topographic correction, but a few artifacts still remain. Since topographic-correction modeling is done with a uniform model resistivity, correcting for topographic effects in a separate step does not include the interaction between topography and subsurface resistivity structure. The topographic-correction approximation gets less accurate as subsurface resistivity contrasts increase.

Imaging can be refined further by combining topography and resistivity structure modeling in the inversion procedure. Simultaneously modeling both topography and geologic structure removes the assumption of an uniform background resistivity made when topographic effects are modeled separately. Figure 10a shows a smooth-model section created by inversion of uncorrected fault-scarp data with topography included in the inversion model. Uniform basement and alluvium resistivities are recovered and there is a clear offset in the basement unit. Smooth-modeling broadens the original step-shaped offset into a ramp, but it is centered on the correct location and shows the correct offset. Smooth-model inversion with topography includes the interaction between resistivity structure and terrain, improving the final result.

Topographic Masking

Topographic effects can mask interesting features in apparent resistivity data, making topographic modeling important in areas with significant terrain. To illustrate this point, dipole-dipole apparent resistivity data were calculated for the model section shown in figure 11a. Values were calculated along a line perpendicular to a ridge with a uniform 100 ohm-m resistivity. Calculated apparent resistivities for this ridge model depart significantly from 100 ohm-m, ranging from a low of 26 to a high of 230 ohm-m (figure 11b). As expected, inverting this data set without accounting for topography creates a smooth-model section with spurious structure (figure 12a). Despite significant topographic effects in apparent resistivity, smooth-model inversion with topography recovers the original uniform background resistivity (figure 13a).

Introducing a conductive prism centered at a depth of 120 meters below the ridge top (figure 14a) creates a dipole-dipole apparent resistivity pseudosection (figure 14b) which is similar in appearance to the pseudosection from the uniform background model (figure 11b). Introducing a conductive prism lowers apparent resistivities in pant-legs below the ridge top, but pant-leg positions do not change. Topographic effects are masking the conductor's presence in the apparent resistivity pseudosection. Smooth-model inversion of data from this example removes topographic effects and images the conductive prism, creating a bull's-eye of low resistivity centered 120 meters below the ridge line (figure 15a). Smooth-model inversion shows a conductive feature with limited depth extent at the correct location. Although fine detail is not recovered, smooth-model inversion resolves the location and approximate size of the original conductive prism.

Apparent resistivity data can be strongly distorted by topography, but topographic effects are much smaller in IP data. Adding IP properties to the resistivity model used in the previous example illustrates IP's insensitivity to topography. Figure 16a shows a model section with resistivities supplemented by polarizability properties. Background IP is represented by a uniform 3 mrad, while the conductive prism is given a 50 mrad IP response. Figure 16b shows an IP phase pseudosection calculated for the model shown in figure 16a using a two-dimensional finite element program. A clear triangular pattern, centered on the polarizable prism's location, is present in the IP pseudosection. There is almost no additional character in the IP pseudosection due to topographic effects.

Even when topographic effects are not significant, smooth-model inversion reduces or removes many resistivity/IP pseudosection artifacts, improving the data's interpretability. Inverting the IP data shown in figure 16b creates the smooth-model section shown in figure 17a. Away from the ridge line low background IP phase values are recovered.
Under the ridge line, smooth-model inversion images a compact polarizable object, centered at a depth of 200 meters. Smooth-model inversion collapses the wide triangular dipole-dipole IP pseudosection feature to a compact object much more representative of the original polarizable prism.

Conclusions

Pseudosection plots of resistivity/IP data often have overlapping pant-leg artifacts which make interpretation difficult. Smooth-model inversion provides a way to remove pseudosection artifacts and produce an image section. Smooth modeling can be used as an automated imaging tool by generating a priori starting models with a broad moving-average of observed data. It can also be used as tool for interpretive synthesis by basing a priori models on independent geologic information from mapping, drilling or other geophysical surveys. Topographic effects can distort apparent resistivity data in areas with rough terrain. Using a finite-element forward-modeling algorithm allows for distorted computational meshes which closely follow irregular topographic profiles and accurately model topographic effects. Smooth-model inversion improves the interpretability of resistivity/IP data and in areas with topographic relief, results are improved further by including topographic modeling in the inversion procedure.

References Cited

Dahlin, T., 1996, 2D resistivity surveying for environmental and engineering applications, First Break, v14, p275-283.

Edwards, L.S., 1977, A modified pseudosection for resistivity and IP: Geophysics, v42, p1020-1036.

Loke, M.H., and Barker, R.D., 1996, Rapid least-squares inversion of apparent resistivity pseudosections by a quasi-Newton method: Geophysical Prospecting, v44, 131-152.

Oldenburg, D.W., and Li, Y., 1994, Inversion of induced polarization data: Geophysics, v59, p1327-1341.

Tong, L.T., and Yang, C.H., 1990, Incorporation of topography into 2D resistivity inversion: Geophysics, v55, 354-361.

Tripp, A.C., Hohmann, G.W., and Swift, C.M., 1984, Two-dimensional resistivity inversion: Geophysics, v49, p1708-1717.

Wannamaker, P.E., 1992, IP2DI-v1.00: Finite element program for dipole-dipole resistivity/IP forward and parameterized inversion of two-dimensional earth resistivity structure: Univ. of Utah Research Inst. Rept. ESL-92002-TR.

List of Figures

Figure 1: North Silverbell Line 0 resistivity/IP data.

Figure 2: Smooth-model inversion of North Silverbell Line 0 resistivity/IP data.

Figure 3: Calculated model response for North Silverbell Line 0 smooth model.

Figure 4: Estimated smooth-model error for North SilverBell Line 0.

Figure 5: Tradeoff between fitting observed data and smoothness constraints.

Figure 6: Fault scarp model.

Figure 7: Smooth-model inversion of fault scarp data without accounting for topographic effects.

Figure 8: Topographic correction of fault scarp data.

Figure 9: Smooth-model inversion of topographic-corrected fault scarp data.

Figure 10: Smooth-model inversion, including topography, of uncorrected fault scarp data.

Figure 11: Topographic model with uniform subsurface resistivity.

Figure 12: Smooth-model inversion, without including topography, of topographic model data.

Figure 13: Smooth-model inversion, including topography, of topographic model data.

Figure 14: Topographic model with conductive prism.

Figure 15: Smooth-model inversion of topography plus conductor data.

Figure 16: Topographic model with polarizable, conductive prism.

Figure 17: Smooth-model inversion of topography plus polarizable conductor IP data.

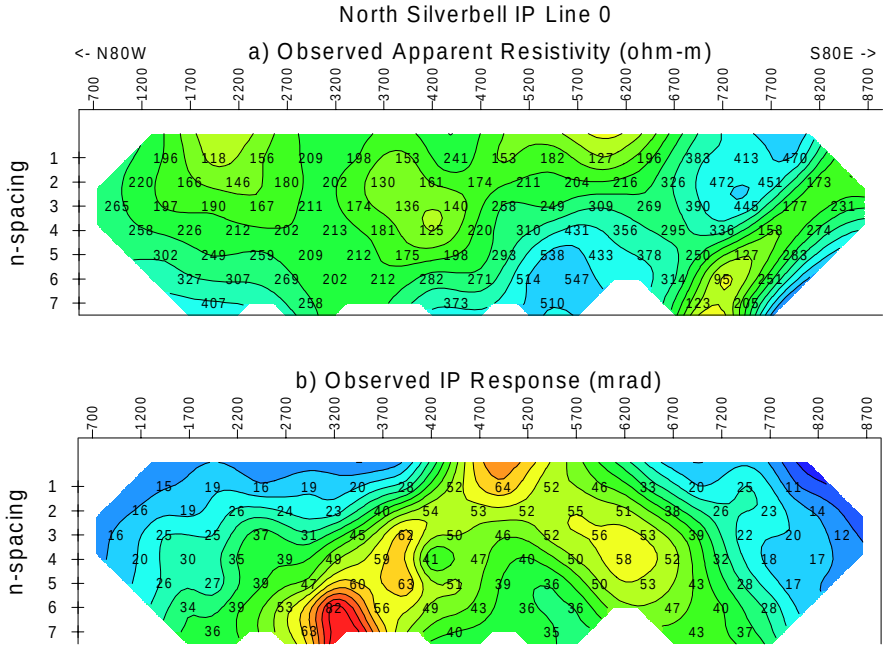

Figure 1. North Silver Bell Line 0 resistivity/IP data. (a) is observed apparent resistivity. (b) is observed IP phase. 500 foot dipole-dipole resistivity/IP data were collected for n=1 to 7.

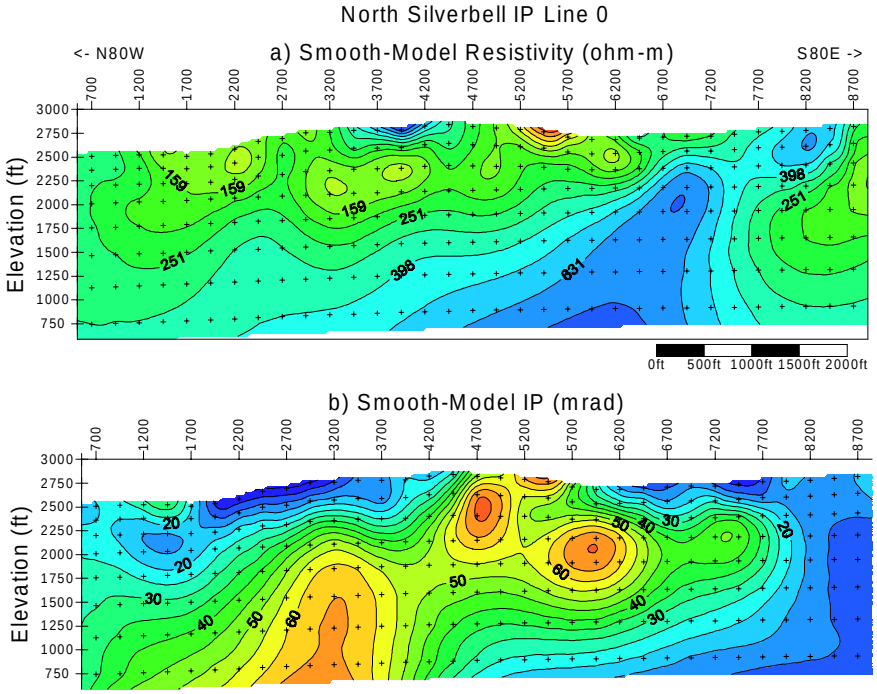

Figure 2. Smooth-model inversion of North Silver Bell Line 0 resistivity/IP data. (a) is smooth-model resistivity section. (b) is smooth-model IP phase section. Smooth-model inversion produces an image-like model section without a pseudosection's pant-leg artifacts.

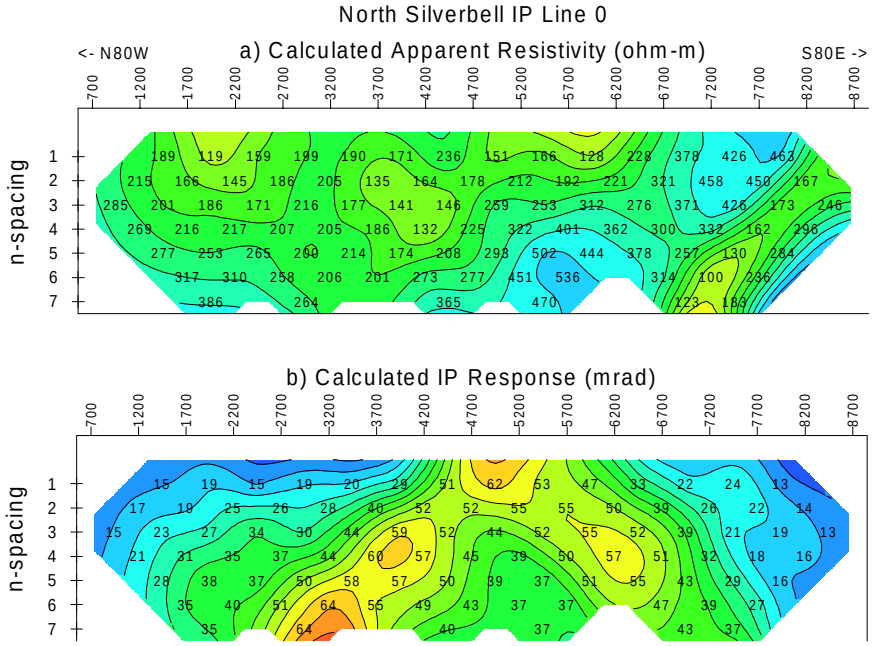

Figure 3. Calculated model response for North Silver Bell Line 0 smooth models. (a) is calculated apparent resistivity. (b) is calculated IP phase. Calculated response closes matches Silver Bell Line 0 observed data (figure 1).

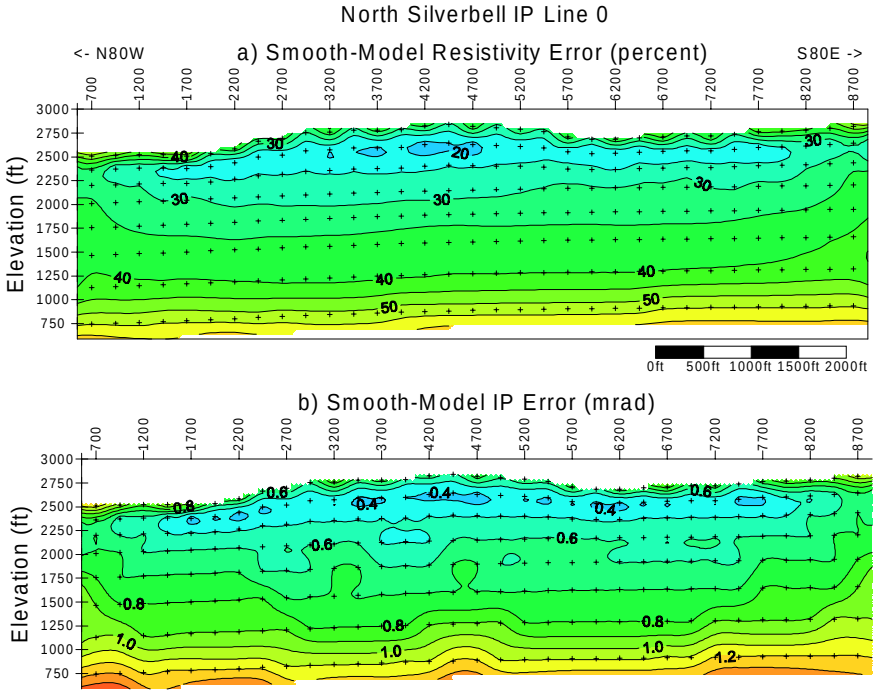

Figure 4. Estimated smooth-model error for North Silver Bell Line 0. (a) smooth-model resistivity error. (b) smooth-model IP phase error. Model error increases below the dipole-dipole array's maximum depth of investigation at n=7.

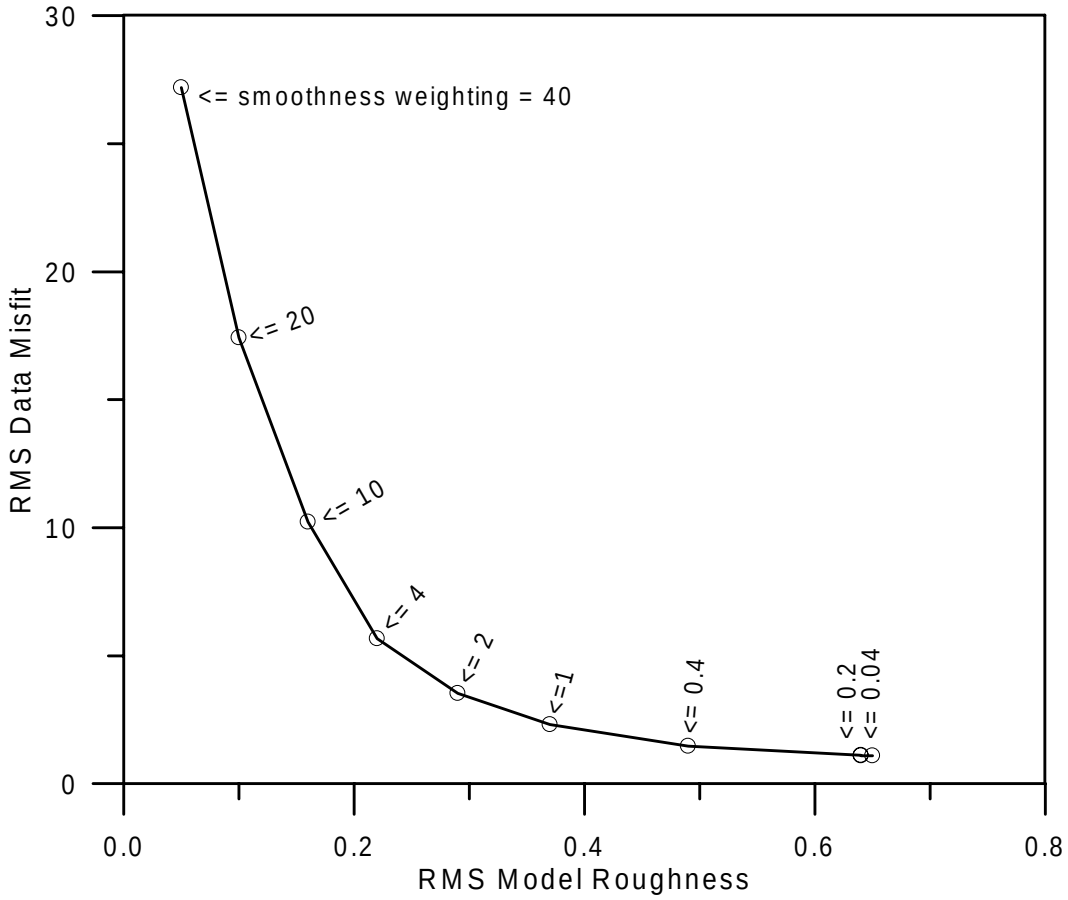

Figure 5. Tradeoff between fitting apparent resistivity data and model-smoothness constraints. Weighting smoothness constraints heavily (smoothness weighting = 40) biases the inversion towards a smooth inversion model which does not fit observed data very well. Unweighting smoothness constraints (smoothness weighting = 0.2) produces a rough model which fits observed data as well as a possible with the inversion model geometry. Choosing an intermediate weight (smoothness weighting=2) optimizes the tradeoff between fitting observed data and keeping the inverse model smooth.

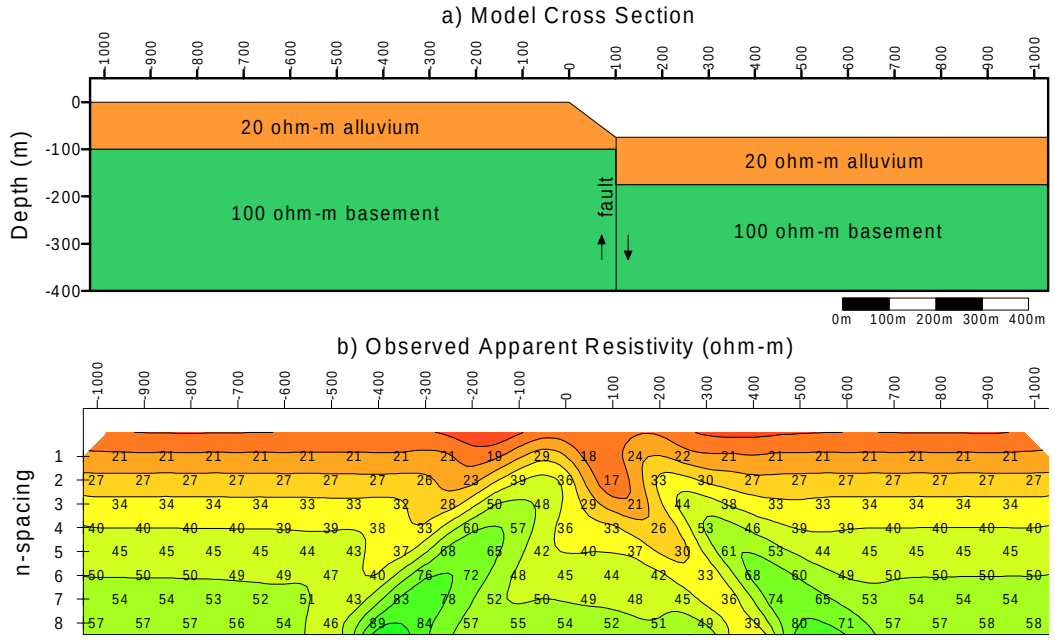

Figure 6. Fault scarp model. (a) is the model section. (b) is a dipole-dipole pseudosection for 100 m dipoles, n=1 to 8, calculated using a finite-element forward model. Topographic effects from the eroded fault scarp mask the response of the basement unit offset. Model adapted from Tong and Yang (1990).

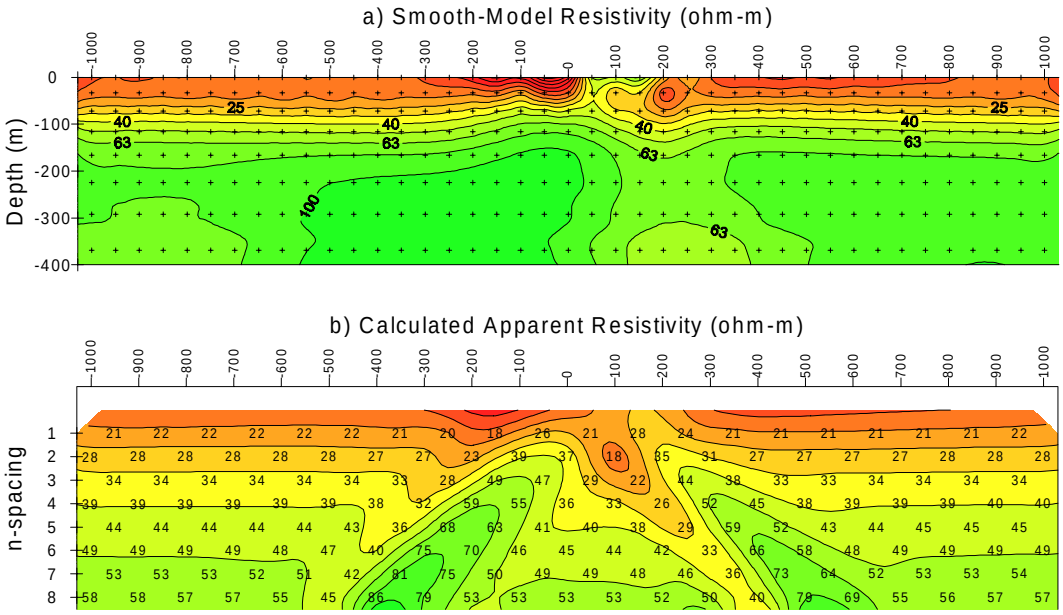

Figure 7. Smooth-model inversion of fault scarp data without accounting for topographic effects. (a) is smooth-model resistivity section. (b) is 100 m dipole-dipole apparent resistivity response of the inversion model.

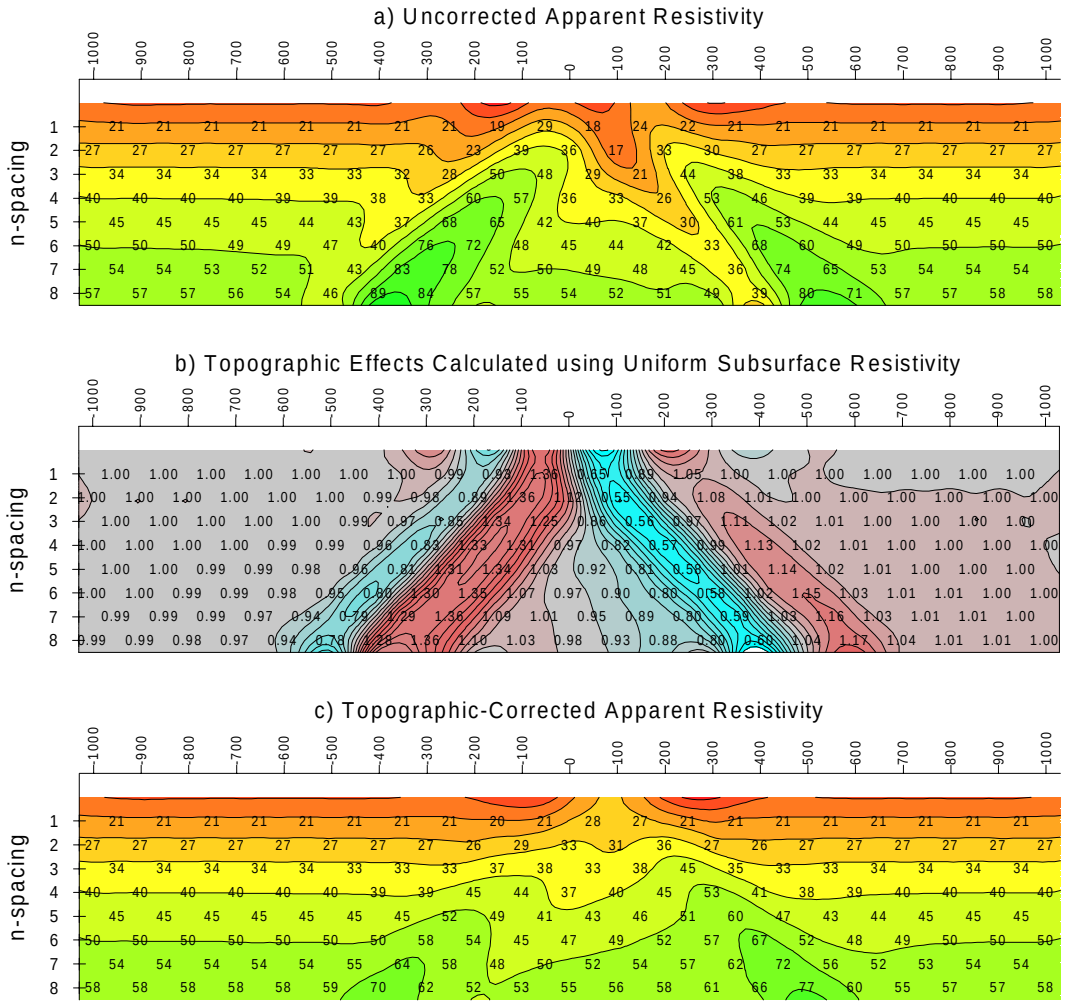

Figure 8. Topographic correction of fault scarp data. (a) is a dipole-dipole pseudosection of uncorrected values. (b) is a pseudosection of terrain effects calculated using a uniform 1 ohm-m subsurface resistivity. (c) is a pseudosection of topographic-"corrected" values created by dividing values in (a) by values in (b).

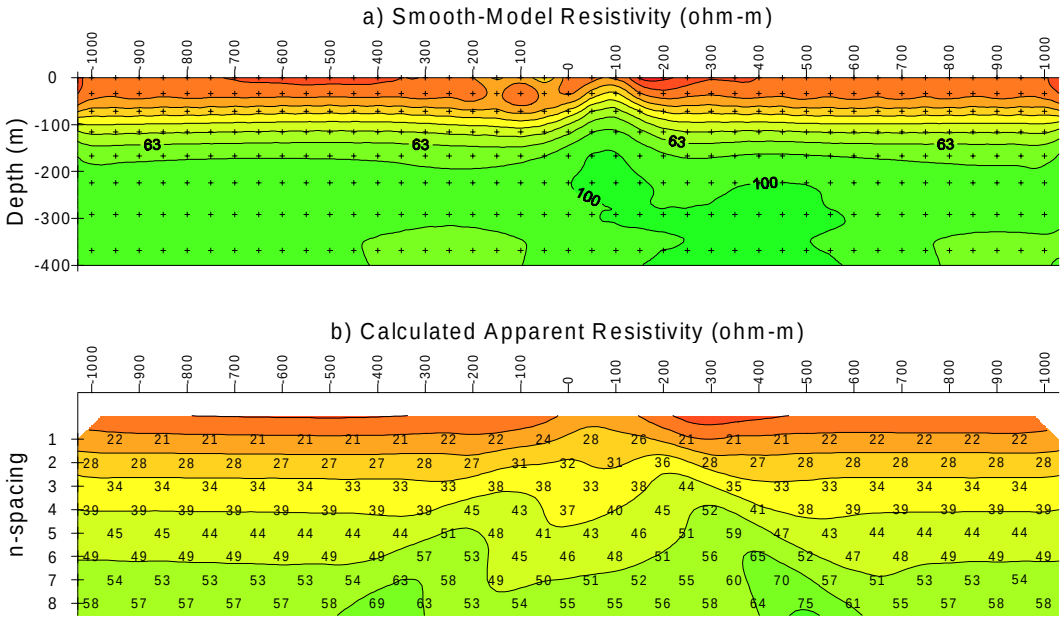

Figure 9. Smooth-model inversion of topographic-corrected fault-scarp data. (a) is smooth-model section. (b) is 100m dipole-dipole apparent resistivity response calculated using inverted smooth model. Topographic correction based on a uniform background resistivity does not remove all topographic effects, so smooth-model inversion is slightly distorted near fault scarp.

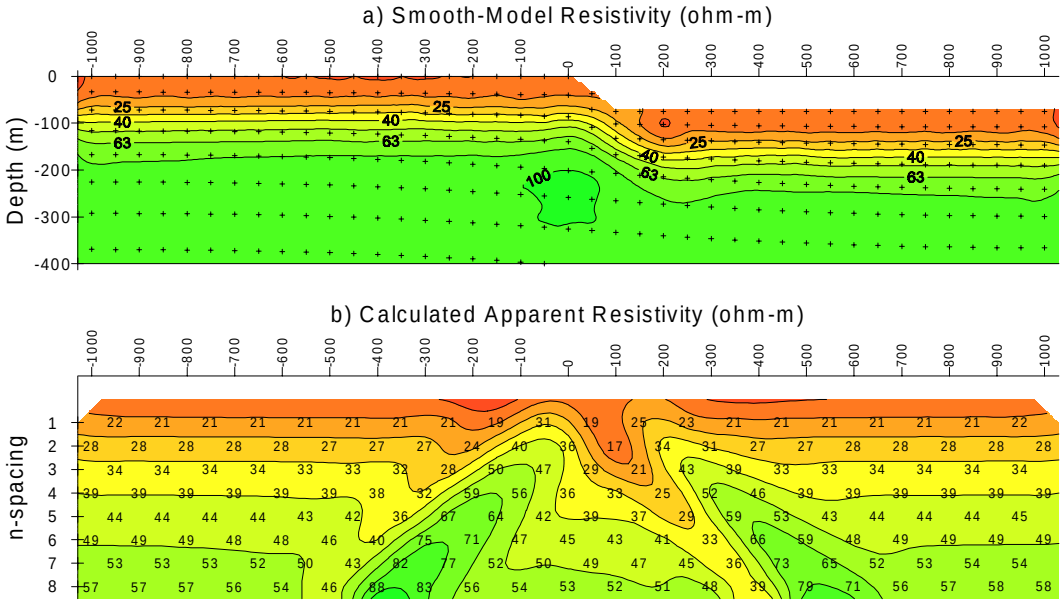

Figure 10. Smooth-model inversion, with topography modeling, of uncorrected fault scarp data. (a) is smooth-model section. (b) is 100 m dipole-dipole apparent resistivity response calculated using inverted smooth model. Smooth-model inversion, with topography modeling, of uncorrected data produces a clear image of the basement unit offset.

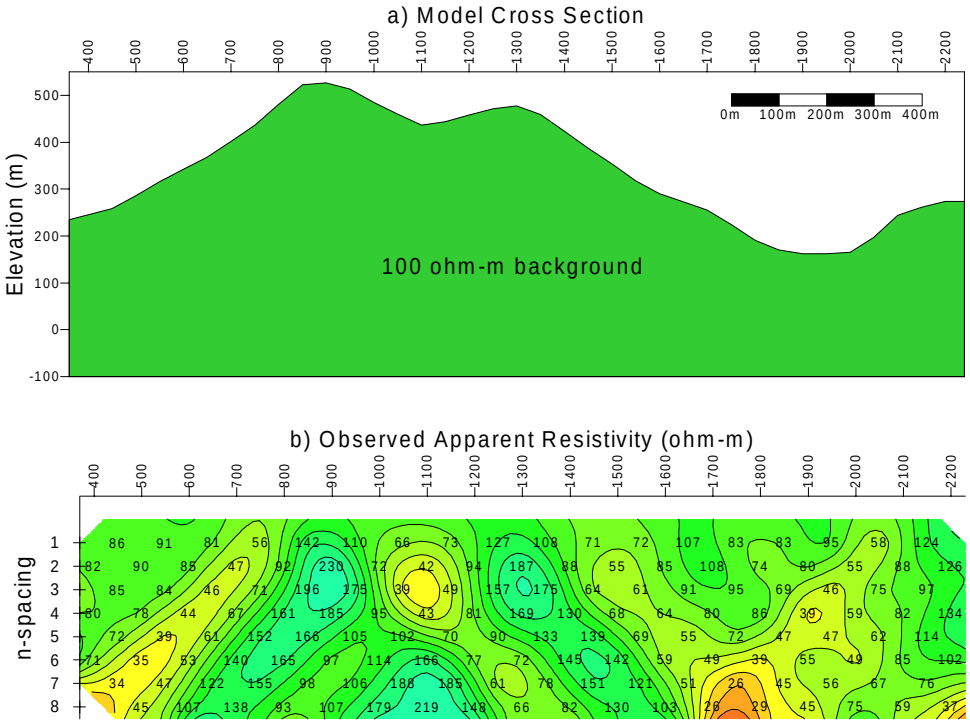

Figure 11. Topographic model with uniform subsurface resistivity. (a) Model cross section. (b) 100 meter dipole-dipole apparent resistivity pseudosection calculated with two-dimensional finite-element forward modeling program. Apparent resistivity data are strongly distorted by topographic effects.

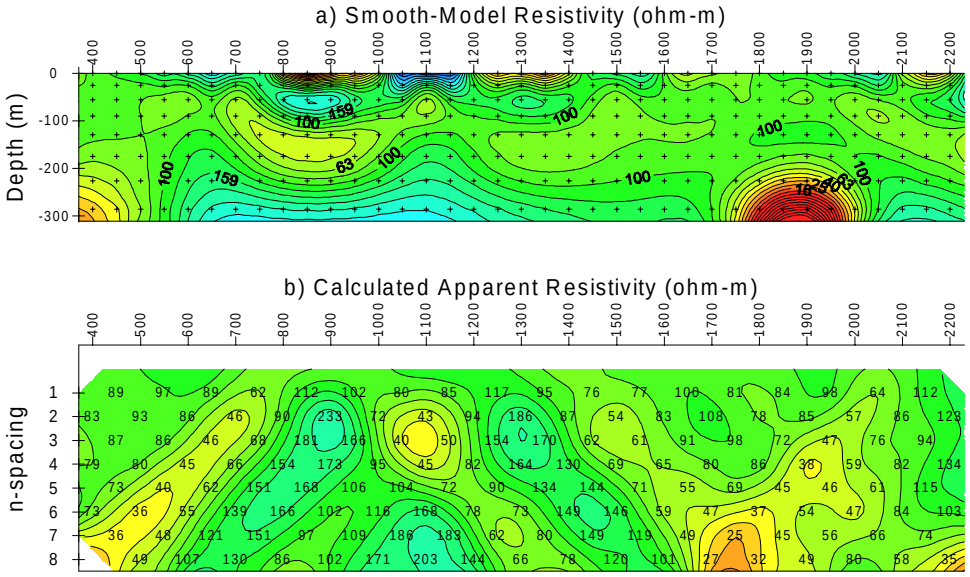

Figure 12. Smooth-model inversion, without including topography, of data from topographic model. (a) is smooth-model section. (b) is 100 m dipole-dipole apparent resistivity response calculated from smooth model. Inverting data without any topographic modeling produces a smooth-model section with spurious structure.

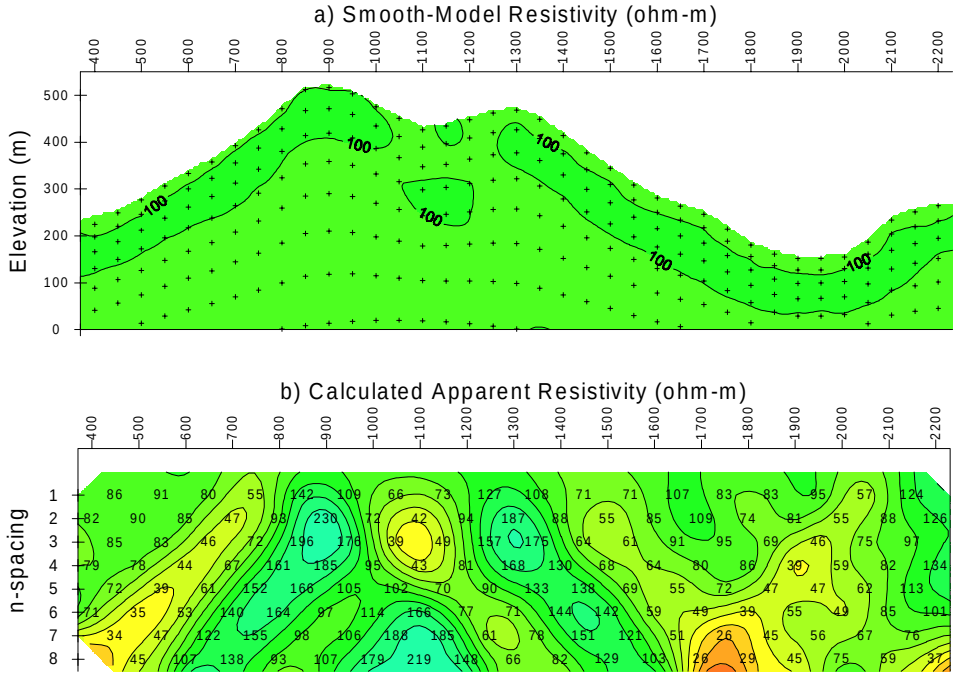

Figure 13. Smooth-model inversion, including topography, of data from topographic model. (a) is smooth-model section. (b) is 100 m dipole-dipole apparent resistivity response calculated from smooth model. Smooth-model inversion with topography recovers original uniform background resistivity.

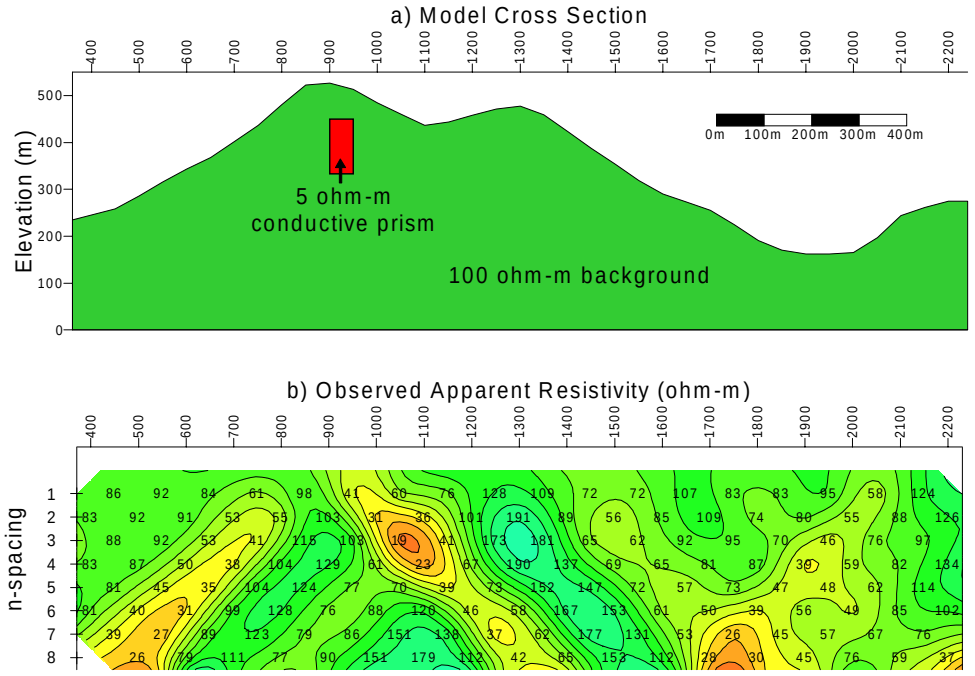

Figure 14.Topographic model with conductive prism. (a) model section. (b) 100 m dipole-dipole pseudosection calculated using two-dimensional finite-element forward model. Topographic effects in apparent resistivity data mask presence of conductive prism, (b) is similar to the pseudosection shown in figure 11b.

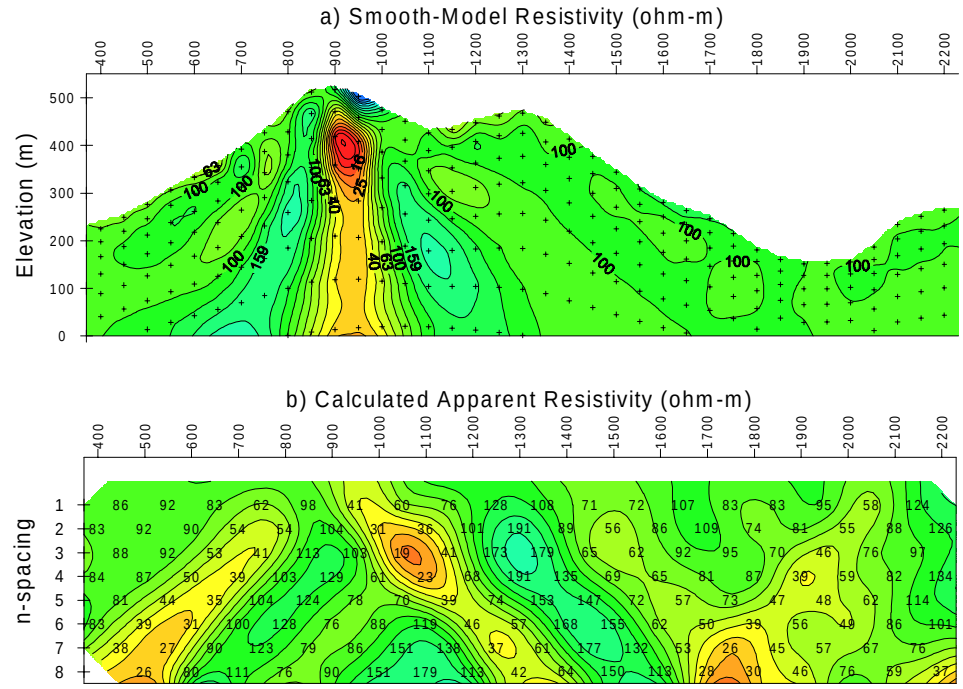

Figure 15. Smooth-model inversion of data from topography plus conductive prism model. (a) is smooth-model section. (b) is dipole-dipole apparent resistivity response calculated from smooth model. Smooth-model inversion with topography suppresses topographic effects and images the conductive prism.

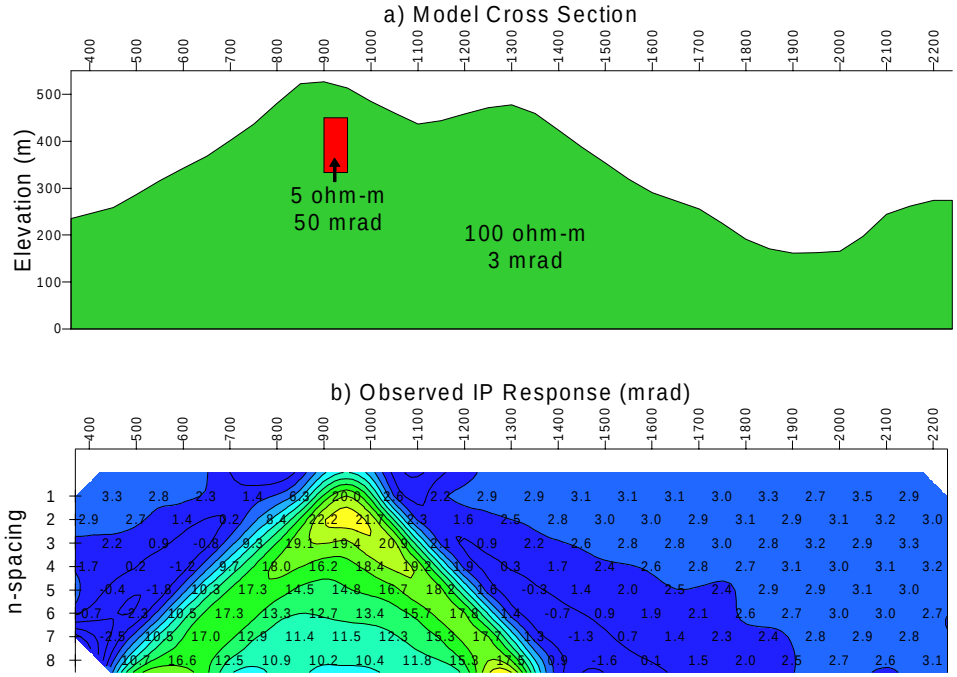

Figure 16. Topographic model with polarizable conductive prism. (a) model section. (b) 100 m dipole-dipole pseudosection calculated using two-dimensional finite-element forward model. IP is much less sensitive to topography than is apparent resistivity.

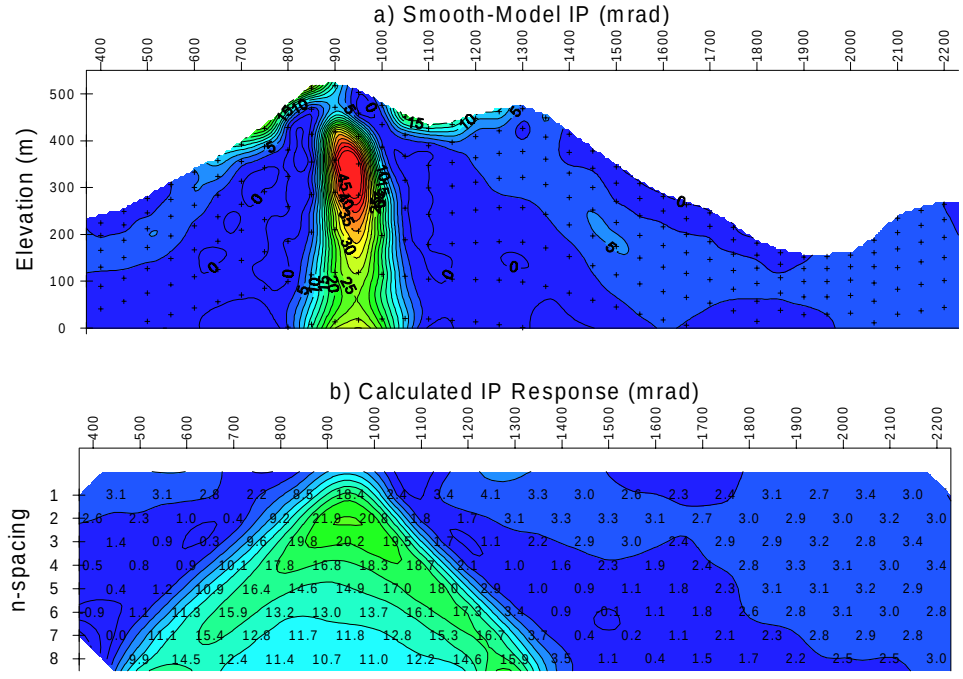

Figure 17. Smooth-model inversion of topography plus conductive prism data. (a) is smooth-model section. (b) is 100m dipole-dipole apparent resistivity response calculated from smooth model. Smooth-model inversion collapses pseudosection pant legs and creates an image-like model section.